Electrochemical and Solid-State Letters, **8** (10) A504-A508 (2005)
1099-0062/2005/8(10)/A504/5/$7.00 © The Electrochemical Society, Inc.

Dual Ion-Beam-Assisted Deposition as a Method to Obtain Low Loading-High Performance Electrodes for PEMFCs

Andrea F. Gullá,[a] Madhu Sudan Saha,[b,*] Robert J. Allen,[a,*] and Sanjeev Mukerjee[b,*,z]

[a]*E-TEK Division of De Nora North America, Incorporated, Somerset, New Jersey 08873, USA*
[b]*Department of Chemistry and Chemical Biology, Northeastern University, Boston, Massachusetts 02115, USA*

Ultralow loading noble metal (Pt) electrodes, for proton exchange membrane fuel cells (PEMFCs), were prepared via dual ion-beam assisted deposition of pure Pt metal particles directly onto the surface of a noncatalyzed E-TEK gas diffusion layer. Activity enhancement, based on normalization with electrochemical surface area and mass activity is reported relative to a commercial gas diffusion electrode containing carbon-supported Pt electrocatalysts. The enhanced performance was primarily dictated by the cathodic oxygen reduction reaction. Based on the morphological differences, which enable such enhanced activities and the mass manufacturability of this electrode system, we report a significant new development in terms of materials for PEMFC application.
 [DOI: 10.1149/1.2008887]

Manuscript submitted April 11, 2005; revised manuscript received June 1, 2005. Available electronically August 4, 2005.

Due to its many advantages compared with other fuel cell systems, there is worldwide interest in the development and commercialization of proton exchange membrane fuel cells (PEMFCs) for vehicular, stationary, and consumer electronics applications. It is well known that, in order for the technology to become commercially viable, the cost of production of the components in a fuel cell and, more importantly, the amount of the precious metal used as the catalyst must be reduced. In this context the role of the membrane polymer electrolyte-electrode interface is crucial, being at the core of the energy conversion process. At this interface efficient transport of ions, dissolved reactants (O_2 and H_2 or gases from reformat output) and products as well as electrons have to be maintained for sustaining high-current densities without reaching mass-transport limitations early on. The introduction of supported platinum on carbon black has already helped lower the platinum loadings of PEMFCs from several milligrams per centimeter squared to about 0.5 mg/cm^2.[1-4] Such a result was obtained by extending the reaction layer interface with the membrane electrolyte further into the electrode.

Further research at Los Alamos National Laboratories was able to bring the cathode platinum loading down to 0.12 mg/cm^2 with very low or negligible loss in fuel cell performance.[5-9] This result was achieved using ink formulations containing supported catalysts and ionomer (typically solubilized Nafion) which was consequently applied either directly on the membrane (using a previously disclosed Los Alamos decal method)[6-9] or on the gas diffusion electrode.[10-15] Using such an approach resulted in a significantly higher catalyst utilizations, thus obtaining a more effective three-phase electrolyte-catalyst-dissolved reactant interface[5,16] within the reaction layer and providing more efficient pathways for ionic and electronic mobility along with the transport of reactants and products.

Among these, early attempts to improve the electrocatalysts utilization was the use of electrodeposition methods, especially the pulse techniques which allowed for selective deposition on active portions of the catalyzed gas diffusion electrode. Among the early reports in this field were those by Taylor et al.[17,18] where higher electrocatalyst utilization was reported as compared to conventional reaction layers with supported catalysts. Low Pt loadings of 0.05 mg/cm^2 were reported with minimal loss in performance when applied as cathodic oxygen reduction electrodes. Subsequently, several reports have shown the efficacy of pulse electrodeposition methods. These include those for controlled deposition of Pt (see recent Ref. 19 and 20 for further details) and Pt alloys.[21,22] Further, formation of metal-polymer composites using pulse electrodeposition of Pt in conjunction with a conducting polymer[23-25] have also been reported. An alternative method, primarily focused on lowering the noble metal requirement has involved spontaneous deposition of Pt on other transition metals resulting in a decoration of nanoparticles with small islands of Pt. Prior work by Wieckowski et al. and Adzic et al. have shown very interesting edge effects resulting in an enhancement of activity.[26,27] Most of these efforts relate to improving catalyst utilization as well as enhanced activity of CO and direct methanol oxidation.

However, in all these advancements the requirement of mass manufacturability with adequate quality control (reproducibility) was questionable at best. To this day, the only effort toward mass manufacturability of a low electrode noble metal loading has been reported by 3M.[28-32] This using a series of vacuum deposition steps with appropriate selection of solvents and carbon blacks results in a nanostructured noble metal containing carbon fibrils which are embedded into the ionomer-membrane interface.[31-33]

Catalyst utilization can also be improved with the use of sputtering techniques particularly when a thin film of about 50 nm of Pt is sputtered onto the front of a standard gas diffusion electrode (GDE) with a supported electrocatalyst reaction layer. Srinivasan et al.[11] studied the effect of such localized platinum on the reaction kinetics. The major contribution from these earlier efforts has been the demonstration of the importance of having a higher concentration of localized platinum at the leading edge of the interface with the polymer electrolyte membrane. Application of these aforementioned approaches for commercial manufacturing has been discussed in a recent publication.[34] The improvement of the reactive layer by sputtering technique on precatalyzed and uncatalyzed electrodes has also been amply investigated by Hirano et al.[35] who surmised that the cathodic performance of a sputtered layer of Pt (0.1 mg/cm^2) can produce results similar to a conventional electrode with a loading of 0.4 mg/cm^2. More recently, Haug et al.[36] have investigated the effect of the substrate on which platinum was sputtered. The best results were obtained with sputtered layers deposited directly on the GDL with optimal performance being those for a 10 nm thick layer of sputtered platinum. Further evidence of this approach is provided by a recent report by O'Hayre et al.,[37] where a sharp increment in performance of a very thin layer of sputtered Pt (5-10 nm) is reported. Power density to the extent of three-fifths of the commercial MEAs (with conventional 0.4 mg/cm^2) is reported with one-fifth the Pt loading. Significant enhancement of catalysts utilization has been also reported in the context of direct methanol fuel cells (DMFC) using the sputter deposition where Pt–Ru alloys were formed by direct deposition on the polymer electrolyte membrane.[38,39]

* Electrochemical Society Active Member.
z E-mail: s.mukerjee@neu.edu

All these prior efforts clearly indicate that alternative deposition methods to the conventionally supported platinum or platinum alloys can be used in PEMFCs having the potential of substantially reducing the total precious metal loading. However, in all these the core issue has been the applicability of the approach to mass manufacturing, cost of manufacturing, and reproducibility of the method. In the last decade there has been a very strong interest in finding alternatives to sputtering techniques in order to improve both deposition and reproducibility. An alternative has been the use of ion beam techniques[40,41] for the direct metallization of polymer electrolyte membranes and/or gas diffusion layers (GDLs) with a catalyst layer for achieving a better catalyst-membrane interface, allowing for better catalyst exploitation and lower noble metal loading while overcoming some of the drawbacks of sputtering techniques. Moreover, extension of these deposition methods represents a promising step towards mass production, thereby enabling further cost reduction and ensuring reproducibility.[42-44]

The objective of this work is to present an application of these ion beam deposition methods via the use of a dual ion-beam assisted deposition (Dual-IBAD) methodology as an improved technology able to produce Pt electrodes having (*i*) better utilization of the precious metal in the reaction layer and (*ii*) very low precious metal (Pt) loading. This technique enables direct coating of a metal layer on a noncatalyzed GDL thus producing in a single step an electrode having very low precious metal loading (0.04-0.12 mg/cm^2 of pure Pt metal) and high fuel cell performance for PEMFC applications. The IBAD technique has been used previously for a very wide range of depositions with varied applications[40,41] and details of the deposition methodology are presented elsewhere.[42] Furthermore, the deposition technique has the advantage of being a low-temperature process, hence easy to scale up because it eliminates the conventional sintering steps required to stabilize the electrode prior to its incorporation in a membrane electrode assembly (MEA). More importantly, it allows production of a catalyst-polymer electrolyte interface entirely composed of metal nanoparticles/nanocrystalline thin film with control in size and distribution, while eliminating the need for a dispersing and supporting medium. Further exploitation of this deposition technique has the potential to initiate the creation of customized products for the micro fuel cell and sensor market. In this communication, we present an ensemble of fuel cell results as well as structure property correlations peculiar to this deposition technique in order to establish the validity of this approach for mass manufacturing ultralow loading Pt-based membrane electrode assemblies.

Experimental

Dual IBAD is a vacuum-deposition process that combines physical vapor deposition (PVD) with ion-beam bombardment. Vapors of coating atoms are generated with an electron-beam evaporator and deposited on a substrate. Ions are simultaneously extracted from the plasma and accelerated into the growing PVD film at energies of several hundred to several thousand electron volts (500 to 2000 eV). Ion bombardment is the key factor controlling film properties in the IBAD process, thus imparting substantial energy to the coating and coating/substrate interface. This achieves the benefits of substrate heating (which generally provides a denser, more uniform film) without degrading its bulk properties. The major parameters of the process are coating material, evaporation-rate, ion species, ion energy, and ion-beam and current density; the influence of all these parameters are described in detail elsewhere.[45-47] In this work, dual IBAD was used to directly deposit onto a commercially available noncatalyzed GDL (LT1400, E-TEK) a layer of pure Pt with prechosen deposition thicknesses of 250 and 750 Å. The ion-beam used power in the range of 500-2000 eV, and the total metal deposited on the GDL had a loading between 0.04 mg/cm^2 to 0.12 mg/cm^2. The gas diffusion layer design consisted of a three-dimensional woven web structure comprised of a carbon cloth support as a substrate with a coating of Teflonized carbon providing for a matrix of (with Vulcan-XC 72 Cabot) and Teflon. Such a GDL has also improved tensile properties and surface roughness which is perfectly suited for superficial metal deposition obtained through IBAD. Comparison was made with respect to conventional electrodes containing supported Pt/C (anode and cathode side), 0.5 mg/cm^2 (each electrode, total loading of 1 mg/cm^2 precious metal) with conventional 30% Pt/C electrocatalysts (commercial electrodes from E-TEK, a division of De Nora North America, Somerset, NJ).

The membrane electrode assembly (MEA) was prepared using a Nafion 112 membrane (DuPont). Prior to MEA fabrication, the membrane was cleaned by immersing in boiling 3% H_2O_2 for 1 h followed by boiling 1 M H_2SO_4 for the same duration with subsequent rinsing in boiling deionized water (1 h). This procedure was repeated at least twice to ensure complete removal of H_2SO_4. The MEA was fabricated in-house via hot pressing ($100°C < T < 140°C$, $5' < t < 10'$, and 200 psig $< P <$ 400 psig. All MEAs were tested in a 5 cm^2 single-cell fuel cell (Fuel Cell Technologies, Albuquerque, NM) using a standard fuel cell test station (built in-house) designed to carry out steady-state polarization measurements. This cell allowed for simultaneous measurements of both single and half cell data with the aid of reference electrodes in the anode chamber (hydrogen reference). The fuel cell test station also allows independent control of humidification, cell temperature, and gas flow rate. All MEAs were conditioned prior to testing using a series of steps; the initial step involved a so-called break-in process in which the cell temperature is slowly raised (approximately 20°C/h) from ambient temperature to the operational (80°C) under N_2. After keeping the cell under these conditions for approximately 5 h in order to allow proper conditioning of the MEA assembly, the pressure was slowly increased to 50/60 psig (anode/cathode respectively). The gases were then switched to saturated H_2/O_2, and the cell allowed to equilibrate for a couple of hours. The cyclic voltammograms (CVs) were obtained using an Autolab potentiostat/galvanostat (model PGSTAT-30, Ecochemie, Brinkman Instruments). Pt wire and a reversible hydrogen electrode (RHE) were used as the counter and reference electrodes, respectively. The CVs were recorded between 0 and 1.2 V in 0.5 M $HClO_4$ at a scan rate of 20 mV/s. The morphological characterization of the electrodes was conducted using scanning electron microscopy/energy dispersive analysis by X-ray (SEM/EDAX) technique (Hitachi field emission SEM/EDAX, model number 5800 with Genesis model 136-10 EDAX containing a Z-max window for lighter elements). The SEM image was observed at different points along the electrode, top surface, and lateral cross section. For the lateral cross section a microtome (Reidhert ultracut model no. E with a diamond knife) with 0.5 μm section size. The energy dispersive X-ray analysis (EDAX) was conducted simultaneously. The EDAX spectrum was recorded at several points along the cross section by moving the sample under the electron-gun, using an X-Y manipulator.

Results and Discussion

To avoid confusion between the various terminologies, the gas diffusion layer (GDL) refers to the noncatalyzed diffuser (LT1400) as described in the previous section, while the terminology gas diffusion electrode (GDE) refers to the catalyzed GDL; whenever we needed the various thickness/loadings of the GDEs that will be clearly pointed out (example, IBAD 750 corresponds to the electrode having a 750 Å thick Pt layer deposited directly onto the standard E-TEK GDL). The loadings corresponding to each of the two different thickness electrodes prepared via IBAD are the following 0.04 mg/cm^2 (IBAD250) and 0.12 mg/cm^2 (IBAD750). Thus when preparing an MEA, the total precious metal loading will be the one obtained by adding the cathodic and anodic sides of the cell (example, the MEA comprised of the IBAD750 will have a total precious metal loading of about 0.24 mg/cm^2).

X-ray diffraction (XRD) spectra.— The XRD patterns for the IBAD GDEs and of the noncatalyzed GDL are shown in Fig. 1. The

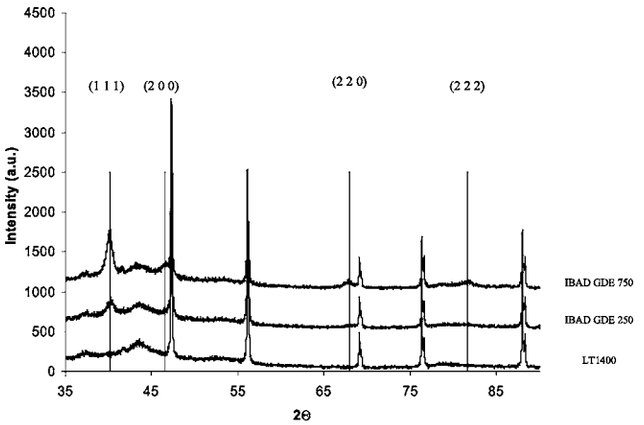

Figure 1. XRD patterns of the noncatalyzed GDL (LT1400) compared to the prepared electrodes (IBAD250, and IBAD750 having precious metal loadings of 0.04 mg/cm^2 and 0.12 mg/cm^2, respectively).

lines from the diffraction of Pt are superimposed on the background represented by the noncatalyzed GDL as well as to the internal sample reference (Si, showing the characteristic five sharp peaks used in this case to align the various diffraction patterns). The X-ray patterns shown in Fig. 1 clearly indicates that increased loading results in further enhancement of definition/resolution of each one of the Pt diffraction peaks. Judging from the spectroscopic features represented by (111) diffraction peak ($2\Theta = 39.764°$) and using the peak width at half intensity (Scherrer treatment), the crystalline size of the diffracting domains range in size between 90 and 100 Å (or 9.0/10 nm). Discussion of the remaining peaks present will be the subject of a more detailed paper wherein the relative population of various crystalline faces in the IBAD deposits will be compared to those typically encountered in supported catalysts. However the important distinction here is that the size of the diffracting domains is larger (90 to 100 Å) than those typically encountered in supported Pt/C where the range of particle sizes is 25-40 Å. These larger particle sizes represent a shift toward greater relative population of bulk crystalline faces on the surface as compared to supported Pt crystallite on carbon. Further, in contrast to supported Pt/C where small particles of Pt are typically embedded into a porous network of carbon support thus providing for a porous network of reaction centers on a conducting substrate, IBAD represents a coating of Pt onto the top porous carbon layer of the noncatalyzed GDL. From these the key differences are (*i*) the presence of higher proportion of bulk crystalline faces on the IBAD deposited surface and (*ii*) the fact that the IBAD deposits are not imbedded into porous carbon blacks, instead they represent top layer deposits. The global availability is higher despite the lower surface area manifested by the larger particle size.

Scanning electron microscope (SEM) measurements.— Figure 2 shows the SEM micrographs taken for noncatalyzed GDL (Fig. 2a) and after metallization, the IBAD750 GDE (Fig. 2b) with a magnification of 50,000 times. Pt deposition at the top surface of the noncatalyzed electrode is evident from the difference in contrast to Fig. 2b. This comparison clearly indicates that the porous nature of the noncatalyzed electrode remains unchanged as a result of the IBAD deposition. This is important from the perspective of mass transport of proton and dissolved reactants to the IBAD deposits (reaction centers). Further Fig. 2c and d show the nature of these IBAD deposits from the perspective of the electrode cross section as represented by 250 and 750 Å deposits, respectively. As noticed from these cross sections, the deposits are primarily limited to the top surface of the GDL; the increase of the thickness of the deposits between 250 and 750 Å is clearly evident. Further analysis of this cross section using EDAX will be presented in the full version of this paper. However from a qualitative perspective it is evident that the increase of the deposition thickness (as represented here using a comparison of 250 and 750 Å IBAD electrodes includes both an

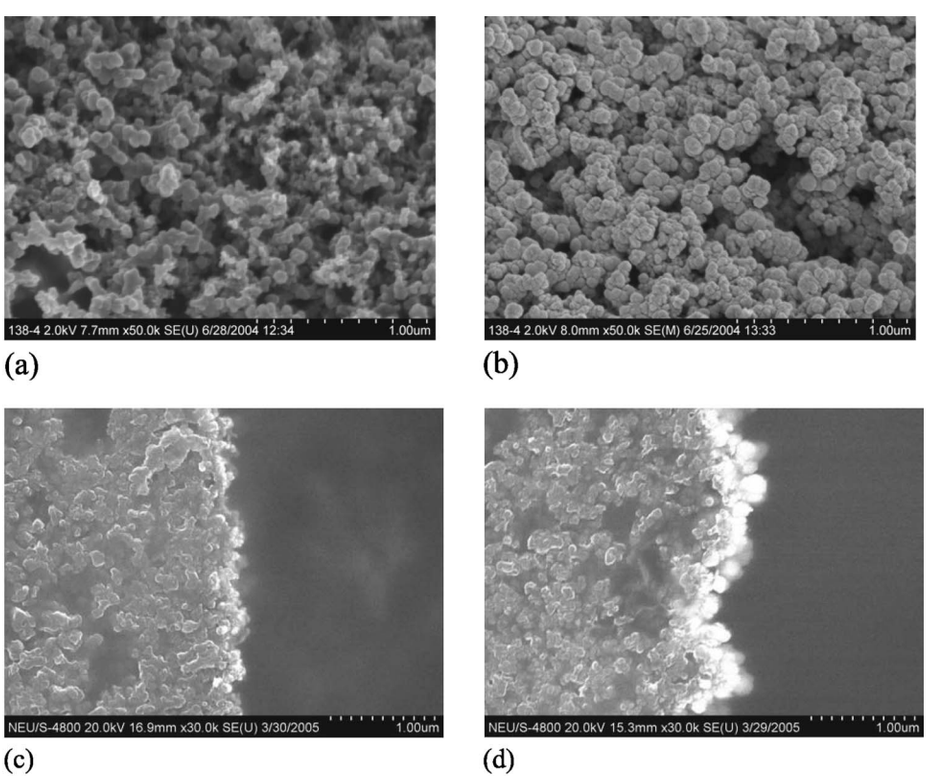

Figure 2. (a) SEM micrograph of the noncatalyzed GDL (LT1400) compared to the (b) micrograph of the IBAD250 having an electrode loading of 0.04 mg cm^{-2}. Cross section of IBAD electrodes are shown for (c) 250 Å and (d) 750 Å IBAD electrodes. Note that the Pt deposits are represented by the lighter contrast in the SEM pictures. In addition the Pt deposits on carbon are independent of the extent of their penetration into the electrode structure. The SEM pictures in (c) and (d) reflect the penetration depth and not the thickness of the deposits.

Table I. Electrode kinetic parameters for oxygen reduction on the IBAD and standard E-TEK GDEs. Charge-transfer resistance was obtained using impedance analysis in a single cell with H_2/O_2 flow at open circuit potential.

Electrode	E_o (mV)	b (mV/decade)	$I_{900\ mV}$ (mA/cm^2)	$I_{900\ mV}$ (mA/mg)	$I_{850\ mV}$ (mA/cm^2)	$I_{850\ mV}$ (mA/mg)	S_{EL}[a] (cm^2/cm^2)	A_{EL}[b] (m^2/g$_{cat}$)
IBAD250	1033	70.8	37.5	937.5	146.4	3660.0	26.0	65.0
IBAD750	1055	64.5	102.8	856.7	447.7	3730.8	35.5	29.6
E-TEK[c]	1043	56.4	110.4	220.8	571.7	1143.4	91.2	18.2

[a] S_{EL}: real surface area obtained electrochemically.
[b] A_{EL}: real surface area obtained electrochemically per gram of catalyst.
[c] 0.5 mg/cm^2 Nafion solution loaded.

increase of the depth of penetration into the GDL structure and an increase of the density of Pt at the top surface. Finally, the fact that in the case of the IBAD, the deposits are primarily at the top surface of the electrode (as shown here), they represent a very different MEA configuration as compared to the conventional MEAs with supported electrocatalysts, in the latter the motivation is to extend the electrochemical polymer electrolyte-electrode interface further into the electrode reaction layer. In the IBAD structures, however, the interface is pushed further toward the immediate interfacial zone with the polymer electrolyte membrane.

Electrochemically active surface area and catalyst utilization.— The electrochemically active surface area of the IBAD (250 and 750 Å) and standard E-TEK GDEs were estimated from the integrated charge in the hydrogen desorption region of the CVs. The areas (m^2/g) were calculated assuming a correspondence value of 0.21 mC/cm^2, obtained using a surface density[48] of 1.3 $\times$ 10^{15} atom/cm^2, and accordingly to the equation

$$A_{EL}(m^2\ g_{cat}^{-1}) = Q_H/(0.21 \times 10^{-3}\ C g_{cat}^{-1})$$

The calculated values of roughness factors (cm^2/cm^2) as well as roughness factors normalized on the basis of Pt loading (cathode electrode, see the next section for details) are listed in Table I.

Steady-state polarization behavior in PEMFCs.— For comparison of the performance of PEM fuel cells, activity for the cathodic oxygen reduction reaction was considered exclusively. This was based on the fact that the anodic half-cell behavior for IBAD (250 and 750 Å) as well as the conventional electrode with supported catalyst (0.5 mg/cm^2) exhibited the same kinetics on a geometric surface electrode area basis, without need for IR correction, etc. This comparison is shown in Fig. 3. Hence all the cell polarization curves primarily exhibited the activity changes due to cathodic oxygen reduction reaction.

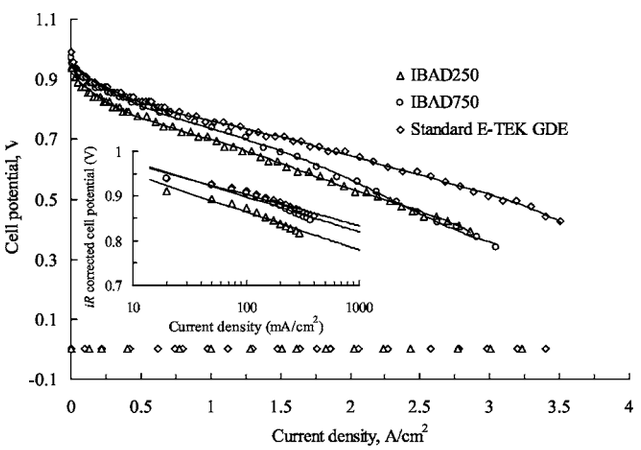

Figure 3. Cell potential vs current density plots for the MEAs prepared using IBAD250 and IBAD750 (both anode and cathode) without Nafion impregnation at 80°C, Nafion 112 membrane, 50/60 psig anode, and cathode back pressure. The standard E-TEK electrode (LT140E-W; 0.5 mg/cm^2) is used for comparison with a standard Nafion loading of 0.5 mg/cm^2. Inset in the figure shows the corresponding IR corrected Tafel plots for comparison of kinetic parameters (Table I). Also shown is the comparison of the half-cell polarizations for all electrodes measured under the same conditions.

In the context of the cathode electrodes, for IBAD electrodes a change from 250 to 750 Å deposition causes a corresponding increase in the electrochemical surface area (cm^2/cm^2, roughness factor) to 27%, the corresponding change in the activity (at 0.9 V vs RHE) normalized with respect to real surface area, is ~50% (Table I). From the perspective of a corresponding comparison with the mass-normalized electrochemical surface area (m^2/g catalyst), while there is an expected lowering of surface area (~54%), a concomitant lowering of mass activity is ~8.6%, (at 0.9 V vs RHE) which is just above the level of error inherent in these measurements (approximately 5% in the range 0.75 to 0.9 V vs RHE) (Table I). Comparison with values obtained at 0.85 V vs RHE shows a similar trend for both (Table I), though numerically there were some differences. Comparison with the control, E-TEK (Pt/C,0.5 mg/cm^2) with IBAD 750 Å electrode, shows a 61% increase in the electrochemical surface area for the E-TEK electrode, the corresponding change in the activity (at 0.9 V vs RHE) normalized for real surface area shows a drop of 57% for the E-TEK electrode as compared to IBAD (750 Å) (Table I). A similar comparison based on mass specific area and activity shows that there is a lowering of mass-normalized electrochemical surface area for the E-TEK electrode relative to the IBAD (750 Å) electrode to the extent of 38.5%, however, the mass-normalized activity comparison shows a more significant drop for the E-TEK electrode (relative to IBAD 750 Å) to the extent of 74.2%. This is significant from the perspective of the new deposition method as our comparison indicates a more effective catalyst utilization as well as enhanced activity. This enhanced activity for the IBAD structure is the subject of a more comprehensive discussion in the full version of this manuscript. The different topology of the IBAD deposits has an important role to play in this context.

Conclusions

Dual ion-beam assisted deposition was successfully used to prepare platinum electrodes for PEMFCs. The results show that according to this methodology, it is possible to deposit thin layers of Pt on carbon electrode substrates with varied loadings without significantly altering the porous carbon electrode structure. The morphology of the deposits is very different from those typically encountered in carbon-supported Pt electrocatalysts, both from the perspective of the relative population of the surface crystalline planes as well as particle size. This method for preparing electrodes relies on concentrating the reaction zone closer to the polymer electrolyte-electrode interface instead of attempting to extend the interface further into the electrode reaction layer, the latter being the motivation behind the use of supported electrocatalysts such as the

E-TEK electrode used in this work (control). The comparison of cell polarization characteristics represented the oxygen reduction activities as the anode polarization was negligible (as expected) and remarkably similar for both E-TEK and IBAD electrodes. The cathode activity comparison indicates the significant advantage for the IBAD electrodes both from a real surface area and more importantly from the perspective of the mass-specific activities. Thus this communication shows a commercially viable process was able to produce (by mass manufacturing) a low noble metal loading electrode with very superior activity in the PEM fuel cell context. The full paper will discuss further the details of electrocatalysis in the context of this new deposition method.

Acknowledgments

This work has been sponsored in part by the Department of Energy grant DE-FC04-02AL67606, and it is registered with the Office of Patents and Trademarks under the following numbers: 6,077,621, 6,673,127, 6,017,650, and 6,103,077. The authors wish to gratefully thank Dr. Enrico Ramunni (De Nora Tecnologie Elettrochimiche S.r.l., Italy), Dr. Emory S. De Castro (E-TEK Division of De Nora North America, Inc.) for their constructive observations during various phases of the project.

Northeastern University assisted in meeting the publication costs of this article.

References

1. E. A. Ticianelli, C. R. Derouin, A. Redondo, and S. Srinivasan, in *Electrode Materials and Processes for Energy Conversion and Storage*, S. Srinivasan, S. Wagner, and H. Wroblowa, Editors, PV 87-12, p. 166, The Electrochemical Society Proceedings Series, Pennington, NJ (1987).
2. E. A. Ticianelli, C. R. Derouin, A. Redondo, and S. Srinivasan, *J. Electrochem. Soc.*, **135**, 2209 (1988).
3. E. A. Ticianelli, J. G. Beery, and S. Srinivasan, *J. Appl. Electrochem.*, **21**, 597 (1991).
4. S. Srinivasan, E. A. Ticianelli, C. R. Derouin, and A. Redondo, *J. Power Sources*, **22**, 359 (1988).
5. M. S. Wilson and S. Gottesfeld, *J. Electrochem. Soc.*, **139**, L28 (1992).
6. M. S. Wilson, C. R. Derouin, J. A. Valerio, and S. Gottesfeld, in *Proceedings of the 28th Intersociety Energy Conversion Engineering Conference*, Vol. 1, 1203 (1993).
7. M. S. Wilson, J. A. Valerio, and S. Gottesfeld, in *Electrode Materials and Processes for Energy Storage and Conversion*, S. Srinivasan, D. D. Macdonald, and A. C. Khandkar, Editors, PV 94-23, p. 145, The Electrochemical Society Proceedings Series, Pennington, NJ (1994).
8. C. Zawodzinski, M. S. Wilson and S. Gottesfeld, in *Proton Conducting Membrane Fuel Cells I*, S. Gottsfled, G. Halpert, and A. Landgrebe, Editors, PV 95-23, p. 57, The Electrochemical Society Proceedings Series, Pennington, NJ (1995).
9. M. S. Wilson, J. A. Valerio, and S. Gottesfeld, *Electrochim. Acta*, **40**, 355 (1995).
10. S. Swathirajan and Y. M. Mikhail, in *Electrode Materials and Processes for Energy Storage and Conversion*, S. Srinivasan, D. D. Macdonald, and A. C. Khandkar, Editors, PV 94-23, p. 158 The Electrochemical Society Proceedings Series, Pennington, NJ (1994).
11. S. Srinivasan, A. Parthasarathy, O. A. Velev, A. C. Ferreira, S. Mukerjee and A. J. Appleby, in *Structural Effects in Electrocatalysis and Oxygen Electrochemistry*, D. Scherson, D. Tryk, M. Daroux, and X. Xing, Editors, PV 92-11, p. 474, The Electrochemical Society Proceedings Series, Pennington, NJ (1992).
12. E. Passalacqua, F. Lufrano, G. Squadrito, A. Patti, and L. Giorgi, *Electrochim. Acta*, **43**, 3665 (1998).
13. R. Mosdale, M. Wakizoe and S. Srinivasan, in *Electrode Materials and Processes for Energy Storage and Conversion*, S. Srinivasan, D. D. Macdonald, and A. C. Khandkar, Editors, PV 94-23, p. 179, The Electrochemical Society Proceedings Series, Pennington, NJ (2004).
14. G. S. Kumar, M. Raja, and S. Parthasarathy, *Electrochim. Acta*, **40**, 285 (1995).
15. A. C. Ferreira and S. Srinivasan, in *Electrode Materials and Processes for Energy Storage and Conversion*, S. Srinivasan, D. D. Macdonald, and A. C. Khandkar, Editors, PV 94-23, p. 173, The Electrochemical Society Proceedings Series, Pennington, NJ (1994).
16. M. S. Wilson and S. Gottesfeld, *J. Appl. Electrochem.*, **22**, 1 (1992).
17. E. J. Taylor, E. B. Anderson, and N. R. K. Vilambi, *J. Electrochem. Soc.*, **139**, L45 (1992).
18. E. J. Taylor, N. R. K. Vilambi, E. B. Anderson, and K. Donohue, in *Structural Effects in Electrocatalysis and Oxygen Electrochemistry*, D. Scherson, D. Tyrk, M. Daroux, and X. Xing, Editors, PV 92-11, p. 540, The Electrochemical Society Proceedings Series, Pennington, NJ (1992).
19. K. H. Choi, Y. J. Park, H. S. Kim, and T. H. Lee, *Hwahak Konghak*, **38**, 1 (2000).
20. S. P. Kumaraguru, H. Kim, and B. N. Popov, in *Proceedings of AESF-SUR/FIN Annual International Technical Conference*, 1054 (2004).
21. B. N. Popov, *Plat. Surf. Finish.*, **91**, 40 (2004).
22. Z. D. Wei and S. H. Chan, *J. Electroanal. Chem.*, **569**, 23 (2004).
23. C. Coutanceau, M. J. Croissant, T. Napporn, and C. Lamy, *Electrochim. Acta*, **46**, 579 (2000).
24. Y.-T. Xu, L.-Z. Dai, Y.-Y. He, R. Tahina, J.-Y. Gal, and H.-H. Wu, *Wuli Huaxue Xuebao*, **19**, 564 (2003).
25. M. T. Giacomini, E. A. Ticianelli, J. McBreen, and M. Balasubramanian, *J. Electrochem. Soc.*, **148**, A323 (2001).
26. J. S. Spendelow and A. Wieckowski, *Phys. Chem. Chem. Phys.*, **6**, 5094 (2004).
27. S. R. Brankovic, J. X. Wang, and R. R. Adzic, *Electrochem. Solid-State Lett.*, **4**, A217 (2001).
28. M. K. Debe, T. N. Pham, and A. J. Steinbach, U.S. Pat. 97,948,851 (1999).
29. M. K. Debe, J. M. Larson, W. V. Balsimo, A. J. Steinbach, and R. J. Ziegler, U.S. Pat. 97,948,627 (1999).
30. M. K. Debe, R. J. Poirier, M. K. Wackerfuss, and R. J. Ziegler, U.S. Pat. 97,948,599 (1999).
31. M. K. Debe, G. M. Haugen, A. J. Steinbach, J. H. Thomas, and R. J. Ziegler, U.S. Pat. 5,879,827 (1999).
32. S. S. Mao, G. M. Haugen, K. A. Lewinski, and M. K. Debe, U.S. Pat. 99,312,514 (2000).
33. Y.-S. Yang, J.-H. Liu, C.-P. Liu, G.-Q. Sun, C.-Z. Li, and T.-H. Lu, *Dianhuaxue*, **6**, 108 (2000).
34. S. Srinivasan, R. Dillon, L. Krishnan, A. S. Arico, V. Antonucci, A. B. Bocarsly, W. J. Lee, K. L. Hsueh, C. C. Lai, and A. Peng, in *Fuel Cell Science, Engineering and Technology*, R. K. Shah, Editor, ASME, New York (2003).
35. S. Hirano, J. Kim, and S. Srinivasan, *Electrochim. Acta*, **42**, 1587 (1997).
36. A. T. Haug, R. E. White, J. W. Weidner, W. Huang, S. Shi, T. Stoner, and N. Rana, *J. Electrochem. Soc.*, **149**, A280 (2002).
37. R. O'Hayre, S.-J. Lee, S.-W. Cha, and F. B. Prinz, *J. Power Sources*, **109**, 483 (2002).
38. C. K. Witham, W. Chun, T. I. Valdez, and S. R. Narayanan, *Electrochem. Solid-State Lett.*, **3**, 497 (2000).
39. B. K. Witham, T. I. Valdez, and S. R. Narayanan, in *Direct Methanol Fuel Cells*, S. R. Narayanan, S. Gottesfeld, and Zawodzinski, Editors, PV 2001-04, p. 114, The Electrochemical Society Proceedings Series, Pennington, NJ (2001).
40. J. K. Hirvonen, *Mater. Res. Soc. Symp. Proc.*, **792**, 647 (2004).
41. T. Hoshino, K. Watanabe, R. Kometani, T. Morita, K. Kanda, Y. Haruyama, T. Kaito, J. Fujita, M. Ishida, Y. Ochiai, and S. Matsui, *J. Vac. Sci. Technol. B*, **21**, 2732 (2003).
42. D. A. Kotov, *Rev. Sci. Instrum.*, **75**, 1934 (2004).
43. F. Pan, F. Zeng, and B. Zhao, *Zhenkong Kexue Yu Jishu*, **22**, 1 (2002).
44. J. Wu, Y. Pan, L. Chen, Y. Zhang, R. Wu, C. Xie, and A. Wang, *Surf. Coat. Technol.*, **176**, 357 (2004).
45. R. J. Allen and J. R. Giallombardo, U.S. Pat. 6,077,621 (2000).
46. C. A. Cavalca, J. H. Arps, and M. Murthy, U.S. Pat. 6,300,000 (2001).
47. M. G. Fernandes, D. A. Thompson, W. W. Smeltzer, and J. A. Davies, *J. Mater. Res.*, **5**, 98 (1996).
48. R. Woods, *J. Electroanal. Chem. Interfacial Electrochem.*, **49**, 217 (1974).